applied sciences

MDPI

Article

Preliminary Study for Smoke Color Classification of Combustibles Using the Distribution of Light Scattering by Smoke Particles

Hyo-Yeon Jang [1] and Cheol-Hong Hwang [2,*]

[1] Department of Disaster Prevention, Graduate School, Daejeon University, 62 Daehak-ro, Daejeon 34520, Republic of Korea
[2] Department of Fire and Disaster Prevention, Daejeon University, 62 Daehak-ro, Daejeon 34520, Republic of Korea
* Correspondence: chehwang@dju.ac.kr; Tel.: +82-42-280-2595

Abstract: Photoelectric smoke detectors are used for early detection of building fires, and sensitivity adjustment is generally performed using white smoke generated by the burning of filter paper. Therefore, when black smoke of the same concentration is introduced, the detector is often not activated. To address this problem, differences in the distribution of light scattered by smoke of various colors were analyzed. A light-scattering chamber with a light-receiving unit for various scattering angles was constructed to measure the scattered light generated inside the chamber of the smoke detector. The light scattering distribution was measured for smoke generated from three combustibles—filter paper (white smoke), kerosene (black smoke), and polyurethane (gray-black smoke)—and three analysis criteria were applied. By identifying a section where the measured values were concentrated for a specific analysis criterion and scattering angle, it was confirmed that some combustibles can be distinguished. Specifically, criterion III, a probabilistic section, was presented to determine which combustible smoke particles were close by applying the proposed section in a complex manner. A preliminary study was conducted to evaluate a methodology for the color classification of smoke particles flowing into a smoke detector chamber; this can be utilized as a foundation for determining optical properties.

Keywords: photoelectric smoke detector; smoke particle; color classification; light scattering distribution; optical properties

check for updates

Citation: Jang, H.-Y.; Hwang, C.-H. Preliminary Study for Smoke Color Classification of Combustibles Using the Distribution of Light Scattering by Smoke Particles. *Appl. Sci.* **2023**, *13*, 669. https://doi.org/10.3390/app13010669

Academic Editor: José António Correia

Received: 1 December 2022
Revised: 26 December 2022
Accepted: 27 December 2022
Published: 3 January 2023

Copyright: © 2023 by the authors. Licensee MDPI, Basel, Switzerland. This article is an open access article distributed under the terms and conditions of the Creative Commons Attribution (CC BY) license (https://creativecommons.org/licenses/by/4.0/).

1. Introduction

Smoke detectors used for the detection of fire in its initial stages can be classified into two types: photoelectric and ionization. These use two different principles to detect fire. However, the production of ionization-type detectors has been halted in South Korea because of radiation concern, and now, only photoelectric-type detectors are used. A photoelectric smoke detector operates by using an LED sensor to detect when the amount of light scattered by smoke particles flowing into the receiver within a sensing chamber exceeds a certain value. This type of detector is in common use because it is inexpensive and relatively simple to install. However, a problem with photoelectric smoke detectors is that their reliability is affected by non-fire aerosols such as dust, steam (water vapor), and aerosols generated in cooking [1,2]. Efforts are, therefore, being made by researchers both within South Korea and elsewhere to prevent such malfunctions, and to identify the characteristics of combustibles to develop complex sensors that can detect heat, smoke, flames, and products of combustion [3,4]. In addition, to detect fire more effectively, smart detectors are being developed that incorporate algorithms for predicting types of combustibles or fire scenarios using machine learning and the Internet of Things (IoT) for data shared in real time [5–7]. However, such sensors are expensive, and they are often impractical, owing to the difficulties involved in maintaining and managing them.

Further, because smoke is influenced in a complex way by factors such as the type(s) of flammable materials and the ventilation conditions, it is a challenge to develop sensors that will satisfy all of the relevant requirements (for economy, practicality, ease of maintenance, and reliability).

Although photoelectric smoke detectors are used for the early detection of general fires, they are intended to detect the white smoke that is initially generated when wood buildings and cotton are burned. Thus, photoelectric smoke detectors used in South Korea are designed by their manufacturers to operate at a certain sensitivity, measured as obscuration per meter (OPM, %/m), in accordance with the "Technical Standards for Detector Type Approval and Product Inspection" [8]. Advantec filter paper No. 2 (Toyo), which generates white smoke upon burning, is used as the source of fire for this sensitivity test criterion. However, in modern buildings, most of the items found indoors are composed of materials such as combustible polymer-based plastics. If the ignition source is such a polymer, black smoke will be generated even at the beginning of the fire, and light scattering by smoke flowing into the chamber of the detector can differ according to the color of the smoke. In other words, when black smoke of the same obscuration threshold is introduced into a detector that operates using scattered light, it can be expected that the sensitivity test will produce inappropriate results. Regarding these photoelectric smoke detector operating characteristics, Jang and Hwang reported on the essential limitation that the OPM designed by the manufacture cannot operate the photoelectric smoke detector at the obscuration threshold generated in a fire, depending on the smoke colors [9]. A detector that operates using light scattering reacts sensitively to white smoke, which scatters more than it absorbs, whereas it reacts more slowly to black smoke, which absorbs more than it scatters [10,11]. Because of this difference in behavior due to smoke color, black smoke introduced into the detector chamber takes longer to detect than white smoke, and this can delay evacuation and expose occupants to danger.

In a South Korean study, the sensitivity of photoelectric smoke detectors was evaluated based on their reaction time when smoke generated from various combustibles was introduced [12]. Jee attempted to distinguish a fire source using scattered-light signals after smoke was introduced into the chamber from multiple angles [13]. Park et al. developed an algorithm to classify patterns of flames and smoke obtained by camera [14]. The algorithm worked according to changes in edge recognition, color difference, and saturation, based on iterated learning of smoke behavior from input images. A sensitivity test has also been conducted on the characteristics of light scattered in the receiver when dust fibers of four colors were introduced into the sensing chamber of a photoelectric smoke detector [15]. Similar studies have been conducted in other countries, including studies in which detector sensitivity was evaluated in terms of reaction time at the moment of detection after smoke from a variety of combustible materials was introduced [16,17]. Wang et al. constructed a multi-angle scatter chamber and analyzed the distribution and optical properties of internally scattered light, according to the type of flammable material [18]. Xie et al. analyzed the light scattering angle according to morphological characteristics by approximating a single particle of white or black smoke using a simple ellipsoid, applying Mie scattering theory [19]. To distinguish between flaming and smoldering, the size of the smoke particle was measured and the optical characteristics were analyzed [20–22]. A variety of optical techniques have been used to analyze the distribution of light scattered in various wavelength bands according to the color, size, and shape of the smoke particles. Recently, classifications by particle size and scattering distribution were evaluated using polarized light [23]. However, it is difficult to establish these variables because fire smoke generation is affected, in a complex way, by the types of flammable materials and the ventilation conditions.

Recently, Deng et al. reported a polarization-based sensor to control the sensitivity of the photoelectric smoke detector's operating time, as the time tends to become delayed or not work because black smoke absorbs light more strongly than it scatters [24]. The idea is to adjust the sensitivity of the detector according to the color of the smoke by making the output similar to the light scattering intensity of white smoke, using a correction factor

for black smoke. Specifically, according to the results of an experiment using standardized materials [25,26], the average scattering intensity of white smoke is approximately four times greater than that of black smoke; therefore, to increase sensitivity, a method that uses a correction factor of 4.0 has been proposed [24]. However, there are a number of limitations in generalizing the optical properties of smoke particles according to particle size and concentration and then applying them to all fire scenarios. This is because the smoke concentration and particle size of the combustion products generated in a fire differ substantially according to the types of combustibles in the actual fire, the ventilation conditions, and the residence times of high-temperature products. Typically, smoke particles grow into agglomerates through complex processes including coagulation, aggregation, breakage, and coalescence [27]. It is difficult to evaluate soot as consisting of uniform-sized particles in a simple burning process, and agglomerates formed between particles cannot be ignored. Further, in a fire with insufficient ventilation, particles actively agglomerate, and it has been reported [28] that the amount of soot generated under this condition can be more than double that in a fire with sufficient ventilation. In summary, defining and evaluating the various phenomena and fire situations (which change in real time) in terms of specific values may provide results that are less reliable than those using a theoretical methodology incorporating sophisticated optical techniques. The consequences can be fatal.

This study was conducted to address the problem of malfunction when black smoke of the same concentration was introduced into the photoelectric smoke detector, whose sensitivity was adjusted to white smoke based on the light-extinction method in South Korea. The optical properties of combustibles producing smoke of various colors were analyzed to activate the detector at the same concentration and reaction time regardless of the smoke color, which depends on the conditions of the fire. In previous studies, the device used for measuring the distribution of scattered light was a complex optical device. However, as a structural change to the smoke detector itself is contemplated, an uncomplicated design is required. Therefore, in this introductory study, the light scattering distribution according to smoke particle color was confirmed using a simple light-scattering chamber (LSC), fabricated in the shape of a photoelectric smoke detector. In addition to providing a reliable report of light scattering distributions, this paper presents a probabilistic indicator developed as the result of repeated experiments. In the end, if an algorithm can be developed that is capable of classifying smoke colors using the characteristics of scattered light measured according to the type of combustible, it will be possible to commercialize it as an enhancement to a smoke detector.

2. Experimental Approaches

2.1. Experimental Method and Procedure

A test duct and light-scattering chamber (LSC) were assembled as shown in Figure 1 to analyze the optical properties of smoke particles generated during the burning of various combustibles. Figure 1a shows the test duct, fabricated in such a way that the smoke particles generated in the experiment follow a particular path. It was made of carbon steel, had a cross-sectional area of 0.3 m $\times$ 0.3 m, and was fastened using rubber packing to prevent smoke leakage. As the specific purpose of the LSC was to measure the distribution of scattered light, burners for smoke generation were installed at the front end, and a Sirocco fan was installed at the rear end. The flow rate was regulated through the fan via an inverter. The P-type fire control panel and test section installed in the test duct were not used in the present study. The test duct was designed such that the smoke generated from the burning combustibles would flow into the LSC by traveling a distance of 2.6 m (calculated as a straight path).

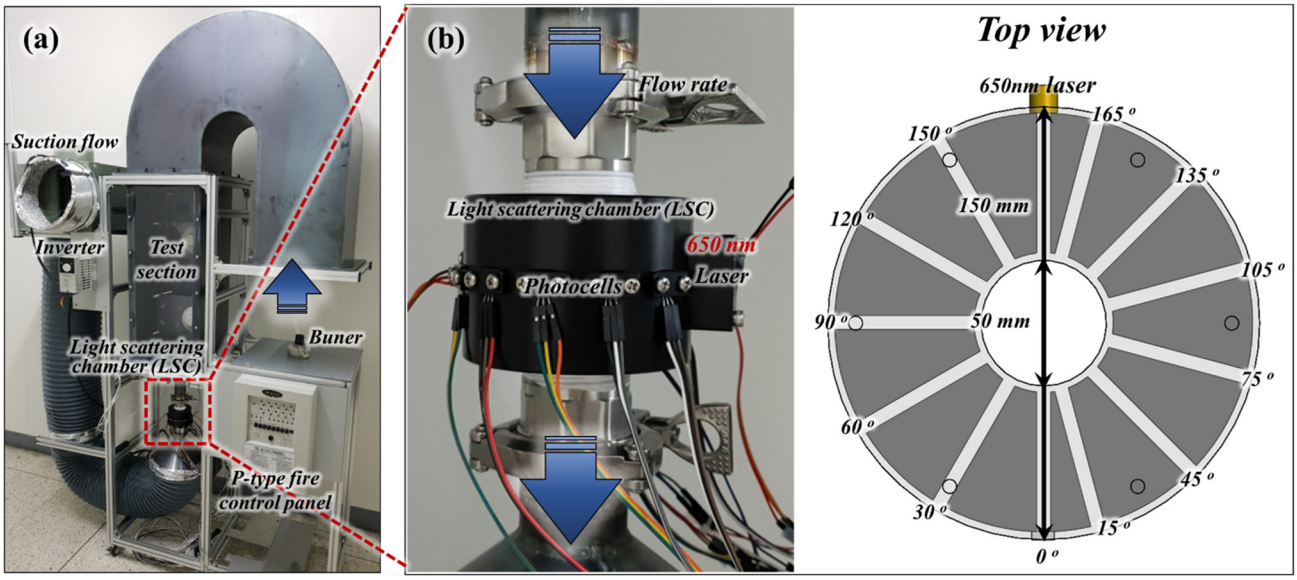


Figure 1. (**a**) Photograph and (**b**) schematics of test duct and light scattering chamber (LSC).

Figure 1b is a photograph and a schematic diagram of the LSC with one light-emitting source and 11 angles, from 0° to 165°, at 15° intervals. When an angle is selected, it is assumed that the light scattering characteristics are axially symmetric to 0° (at which the light transmission signal is measured), following measurement results from previous studies [18]. In the LSC, smoke follows the suction to flow through a 50-mm hole in the center of the chamber. When the smoke particles are exposed to light radiated from the light emitter, the internal light scattering distribution is assessed by measuring the scattered light with its complex characteristics. Within the dark enclosure of the LSC, a black acrylic material was used to block incident light from outside, and 11 photocells in the light emitter (a laser module) and the light receiver (a photocell) were assembled to be in close contact. Specifically, photocells capable of measuring light scattering at 15° intervals were employed to confirm the scatter distribution of optical properties inside the LSC; the light-extinction method [29] was applied using a photocell at 0°. A detailed description of the device and its adaptation was provided by [30]. A wavelength of 650 nm was used, which is the main wavelength used to measure the concentration of smoke particles generated in a fire; this was selected as an initial approach to simplify the interaction between wavelength band size and particle size. The overall design is intended to provide basic information for the determination of light scattering characteristics in this preliminary study, in order to confirm the interaction between the light source and the smoke particles according to various variables.

As the fire source for generating white smoke, shredded filter paper, as used in the sensitivity test, was placed irregularly inside the receptacle so as to generate a sufficient amount of smoke, and flaming combustion was suppressed through the application of an upper plate. For the generation of black smoke, kerosene was applied to a lamp wick, and the smoke concentration was controlled by varying the number of wicks, their diameter, and their exposed length. Finally, for the generation of gray-black smoke, a polymer-based polyurethane (PU) pellet was placed together with methanol onto a rectangular burner, the minimum energy to sustain combustion was supplied, and smoke was generated. The methanol flame supplied sufficient heat for the pyrolysis of the pellet, but the amount of soot generated was very small and, therefore, did not substantially affect the PU smoke concentration. This method has previously been used in evaluating photoelectric smoke detectors; the specific technique for creating a source of smoke is provided by [9].

The principle used to measure the optical characteristics of the smoke particles is based on the light scattering properties of the particles. The conditions for basic analysis are shown in Figure 2. Light scattering refers to the phenomenon in which reflection, refraction,

and diffraction interact in a complex manner [31]; Figure 2a illustrates the scattering as well as the absorption of incident light by smoke particles. The amount of light scattered by the smoke particles is proportional to the amount of radiated light, and may be affected by their size and refractive index as well as the wavelength of the light. According to the basic theory of light scattering, when light reaches the smoke particles, scattering occurs in all directions. Representative of this phenomenon are forms called Rayleigh scattering and Mie scattering. Rayleigh scattering occurs when the size of the scattering particles is smaller than the wavelength of light (e.g., very small water droplets, nitrogen, and oxygen) [32], and Mie scattering occurs when the particle size is similar to or larger than the wavelength of light. Thus, the characteristics of the scattered light vary according to the interaction between wavelength and particle size. As shown in Figure 2b, scattering that occurs in the same direction as the incident light is called forward scattering, and scattering that occurs in the opposite direction is called backward scattering. As the particle size increases, forward scattering becomes more active, and the intensity of light scattered in the light propagation direction increases [33]. To consider this phenomenon in the analysis, the area was divided into two regions—those where forward scattering and backward scattering mainly occur—for the purpose of analyzing the difference between the distributions of scattered light according to the smoke particles introduced into the LSC. For reference, the photocell installed at an angle of 0° serves to transmit the light that is not absorbed or scattered, and the photocell at 90° can be included in both forward and backward scattering.

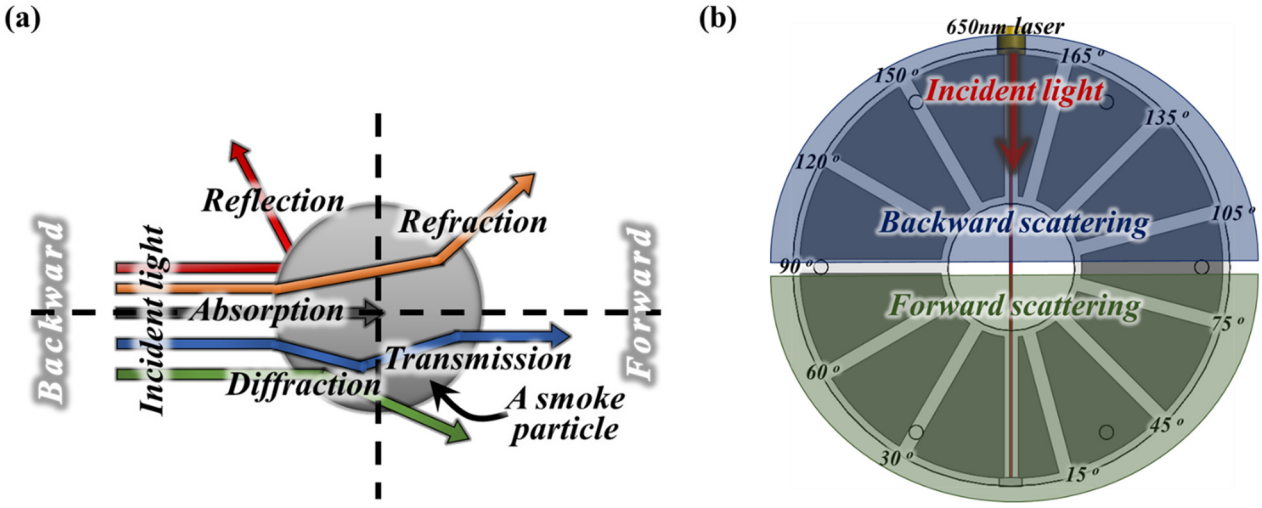


Figure 2. Schematics of optical characteristics: (**a**) schematic of light scattering, absorbed and diffracted for smoke particle; (**b**) schematic of forward and backward scattering inside of a multiple angles chamber.

2.2. Experimental Condition

In our investigation into the intrinsic properties and the optical property distribution of smoke particles, we applied post-processing methods to the acquired data to determine whether it was possible to distinguish between different colors of smoke. Thus, to analyze the scattering characteristics of fire and non-fire beams, as generated in the previous study, the asymmetry ratio, which is the ratio of forward-scattering to backward-scattering angles, was calculated for three types of angles [18,34]. In addition, the single-scattering albedo (SSA) [10,11]—expressed as the ratio of light scattered to light extinction (i.e., sum of scattered and extinction light)—was calculated according to smoke particle color. SSA values closer to 1 indicate that scattering is dominant, and values closer to 0 indicate that absorption is dominant.

These post-processing calculations were performed on all data acquired in the experiment; the three formulas are shown in Table 1 as analysis criteria. The total light extinction and scattering intensity measured in the experiment were analyzed using the initial values for I_i/I_i^0, where I_i^0 was the initial intensity of the light incident from the laser module, I_i was the intensity after the inflow of smoke particles, and the subscript i represented the angle of scattering from 0°. Specifically, criterion I considered the ratio of forward and backward scattering measured inside the LSC to the light extinction signal of 0°, in order to use the SSA and light scattering characteristic in a complex way. With criterion II, forward and backward scattering were evaluated for scattering angles of 15° to 165°, as obtained using the photocells installed inside the LSC, enabling analysis of the asymmetry ratio according to smoke particle color. Lastly, criterion III incorporates the ratio of light scattered to light extinguished according to smoke color for the various angles inside the LSC and the signal measured at 0° (where light is extinction), enabling an examination of the concept of SSA.

Table 1. Analysis criteria of the optical characteristics of combustibles.

No.	Analysis Criterion	
I	$\left\{I_{fs,\,(i)}/I_{bs,\,(180^\circ-i)}\right\}/I_{ext.,\,0^\circ}$	$(i = 15^\circ\sim75^\circ)$
II	$I_{fs,\,(i)}/I_{bs,\ (180^\circ-i)}$	$(i = 15^\circ\sim75^\circ)$
III	$I_{scat.,i}\ /I_{ext.,\,0^\circ}$	$(i = 15^\circ\sim165^\circ)$

I_i: Output voltage according to various photocell installation angles (V). Subscript: '*i*' scattering angle of LSC; '*fs*' forward scatting; '*bs*' backward scattering; '*ext.*' extinction; '*scat.*' scattering.

3. Results and Discussion

3.1. Primary Processing Scattering Light Distribution According to Smoke Particle Color

Figure 3 shows the change in scattering intensity ($I_i - I_i^0$) to confirm the light scattering distribution according to the type of combustibles and the color of the smoke. A repeat calculation method was performed for all experiments to examine the differences, using the optical density (OD, m^{-1}) of the smoke flowing into the LSC. Specifically, the method found the section in which the specific OD was measured for all experimental data, and calculated the average for each combustible. Figure 3a (the results for filter paper smoke,) confirms that a relatively large amount of scattering intensity was measured at 15° and 150°. Figure 3b (the results for kerosene smoke,) shows that light intensity decreased or increased as the optical density increased at specific angles (15°, 150°, and 165°), but there is no consistent pattern at other angles. Figure 3c (the results for polyurethane smoke,) shows a tendency for OD and light intensity to increase proportionally only at angles of 15° and 150°. Because of the characteristics of solid combustibles, not only is it difficult to control the smoke, but the amount of smoke generated is relatively small, making it difficult to perform an accurate analysis. Taken together, these results confirm the degree of change in the primary intensity when smoke particles are introduced into the LSC, and they provide numeric values for the difference in intensity according to the color of the smoke particles from the flammable materials.

In addition, light scattering and extinction were simultaneously measured at 165° because of the LSC characteristics, and kerosene displayed relatively significant photoextinction. This implies that there is a limit to the ability to elucidate the optical properties of smoke particles generated from flammable materials inside the LSC. A photoelectric smoke detector used in a manner similar to this study does not consider the detailed signal of the interaction between the light source and the wall inside the chamber.

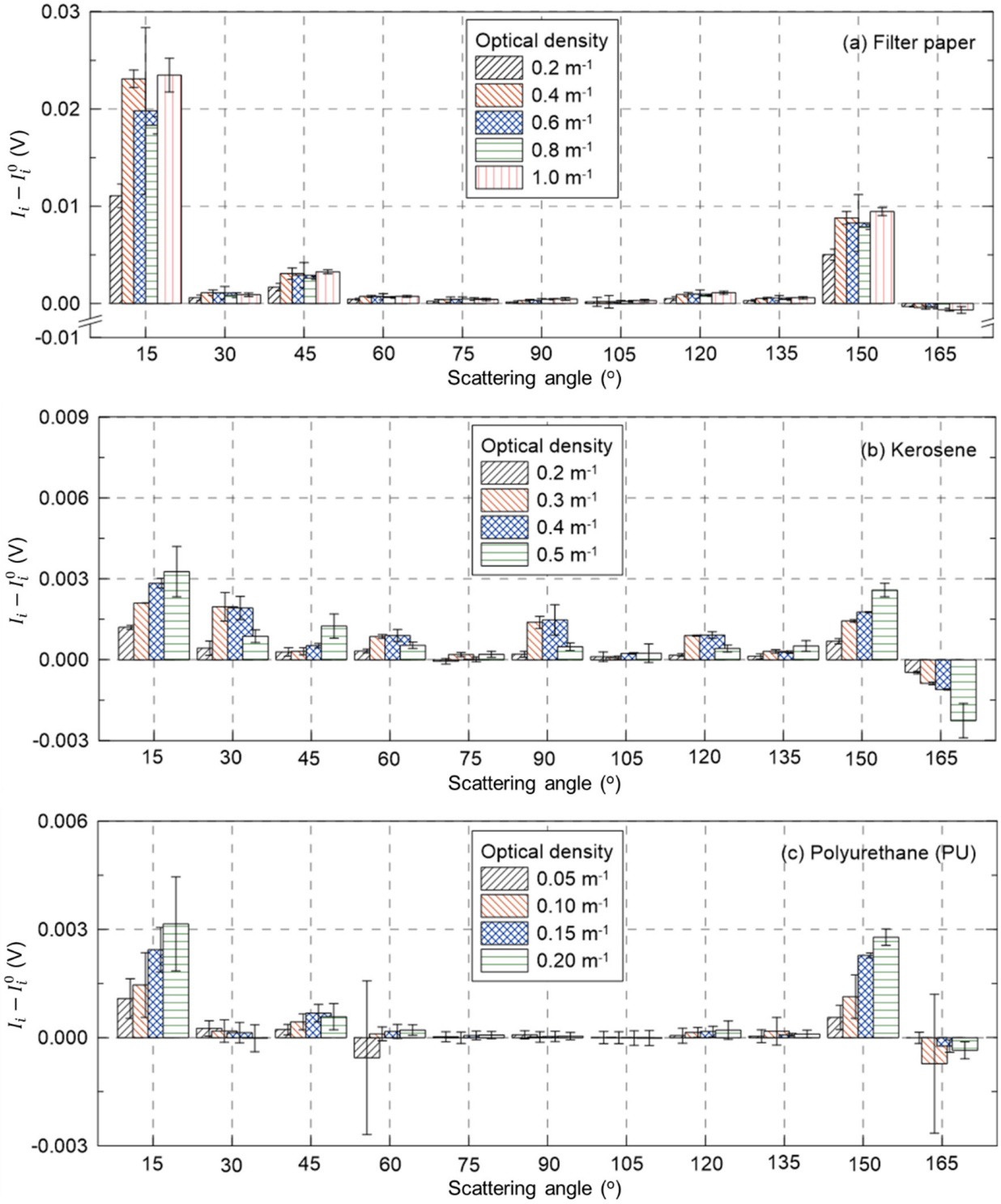


Figure 3. Comparison of experimental data about $I_i - I_i^0$ at LSC on smoke particles.

In order to confirm the absolute change rate (I_i / I_i^0) of the measured value, due to the limitation that the initial value was not measured uniformly in all light receiving units, the result of the dimensionless unit is shown in Figure 4 (excepted 105°). For all three fire sources, the scattered light was relatively strong at 150°, then 15°, then 45°. In addition, it can be seen that the scattered light measurements are fine-grained, and the small figures inserted together are the results of the y-axis scale adjustment at a relative angle that is not clearly confirmed. Figure 4a shows the results for filter paper, and as the smoke is white, the light scattering signal is relatively large. In Figure 4b, the light absorption is found

dominantly at 165° because of the characteristics of kerosene, which produces black smoke. In Figure 4c, a delay appears in the measurement time, because the PU generates a large amount of smoke after the pellet changes to a liquid after being sufficiently heated. As the color of the smoke particles generated from PU was gray-black, a decrease in the signal relative to the initial value of the light-receiving part was, again, observed at 165°.

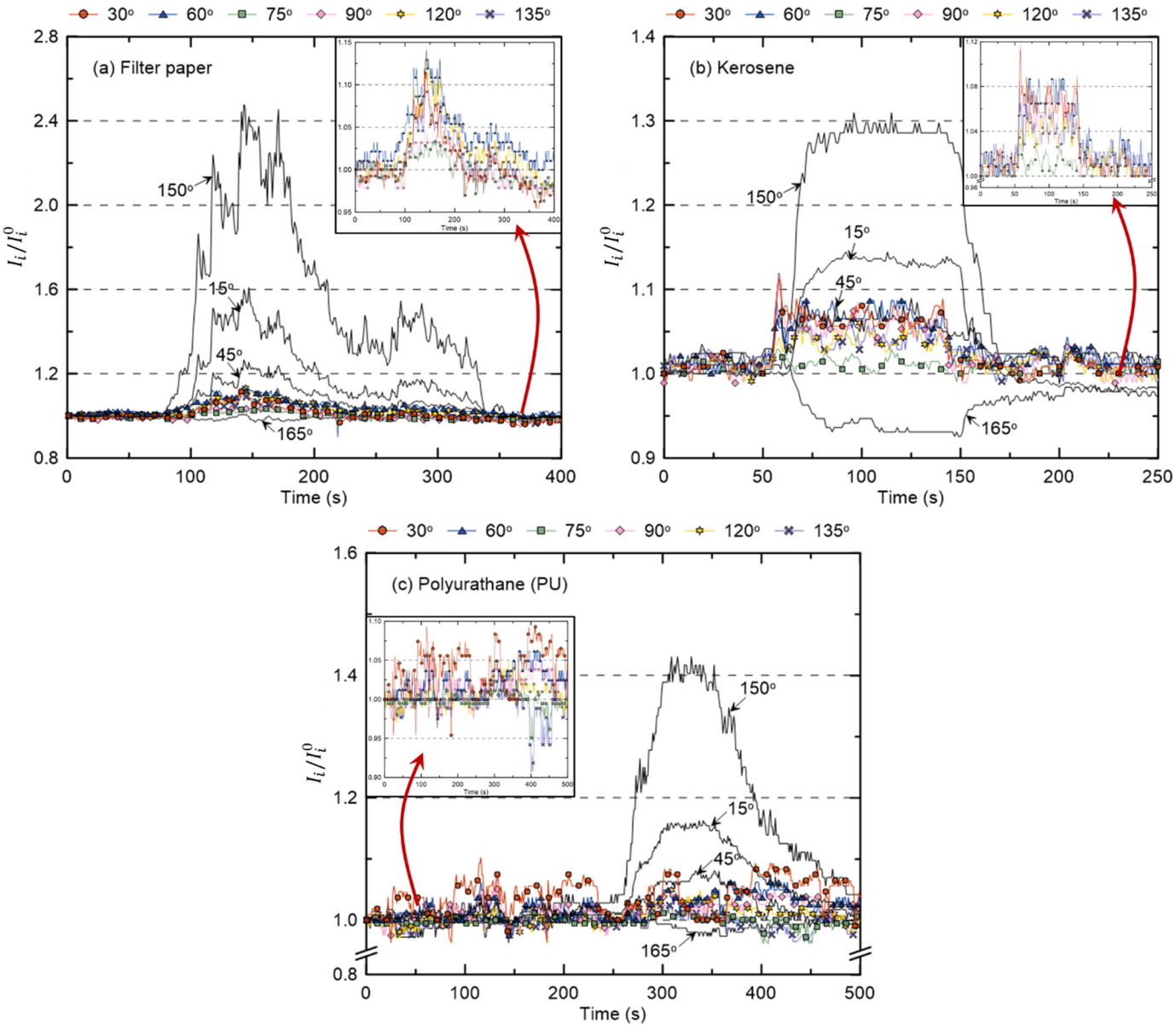


Figure 4. Comparison of experimental data on I_i / I_i^0, measured at LSC on smoke particles.

Figure 5 shows the characteristics of the combustibles and their smoke particles to confirm the distribution of the scattered light for all angles inside the LSC. As mentioned above, this analysis was performed to assess the theory that forward scattering occurs mainly when the smoke particle size is similar to or larger than the wavelength of light. Specifically, the light-distribution scattering ratio (by combustible) is applied to total angles inside the LSC using the post-processed OD of dimensionless. In each plot, the angle axis is divided by 360°, and represents the angular position of the photocell installed in the LSC. In addition, and the radial axis is scaled according to the results for the respective combustibles.

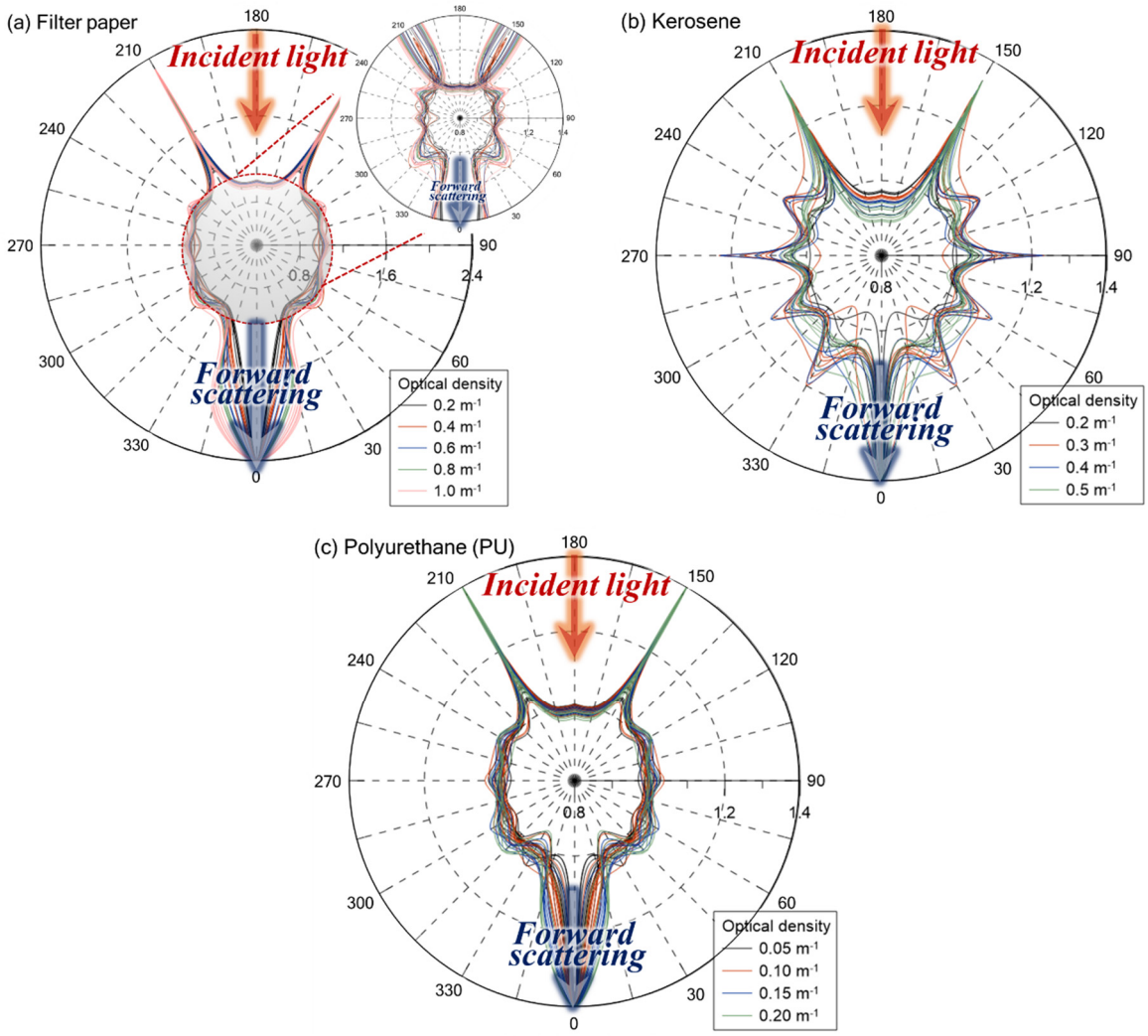


Figure 5. The difference in the distribution of scattering intensity from smoke particles of combustibles.

The results confirm that filter paper (Figure 5a) has high forward scattering relative to kerosene (Figure 5b) and PU (Figure 5c). This finding is predictable based on Mie scattering theory. In addition, the larger the particle size, the greater the diffraction, and based on the report [35] that forward scattering tends to increase and side scattering tends to decrease as total external reflection decreases, it can be inferred that the smoke particles generated from filter paper are relatively large. Specifically, for the combustibles used in this study, the smoke particle size can be analyzed as a ratio of the measured light scattering distribution, and as shown in Figure 5, the magnitude of forward scattering is greater for filter paper than for kerosene or PU. By comparing of the results for kerosene and PU, kerosene is expected to have a smaller particle size, as it displayed side scattering at all angles. However, for light scattering characteristics, wavelength, and particle size, scattering angle, density, shape, and optical material constant (complex refractive index and absorption coefficient) should be considered [36]. In addition, it is difficult to find a clear reason for the agglomerate characteristics of smoke particles generated in a fire, due to their being complex phenomena.

3.2. Post-Processing: Light Scattering Distribution According to Smoke Particle Color, with Criteria Applied

The purpose of this study was to perform a direct comparison between the chamber of a photoelectric smoke detector in actual use in South Korea and the LSC, in terms of the signal inside the chamber representing the light scattering characteristics according to the

color of the smoke particles. To examine the light scattering characteristics inside the smoke detector chamber, it is necessary to consider the concentration of smoke at the moment of activation, because the operating characteristics change according to the color of the smoke generated from the combustibles. To accomplish this, it is necessary to install a photoelectric smoke detector in the same location where the airflow enters the LSC, but this is difficult because of the design of the device. In addition, as the flow at the location of the test section (Figure 1a) was low-speed, the average velocity of the cross-sectional flow entering the interior of the detector changed irregularly. To overcome this limitation in the future, we intend to apply the information derived in previous studies [9] through the use of a fire detector emulator (FDE). Here, the scattering signal measured in the LSC was evaluated together with the information appropriate for identifying the optical characteristics by using the information measured by the fire detector evaluation device, to which the test method was applied through the FDE.

The signal measured at 0° inside the LSC for smoke generated by the combustibles is shown in Figure 6, in the form of OD over time as assessed using the light extinction method. The OD at the moment of detector activation according to the color of the smoke generated by the combustible material was presented for Company J in a previous study [9]. As shown in the figure, at the time of detector activation, the OD of white smoke generated from filter paper was 0.104 m^{-1}, that of black smoke from kerosene was 0.203 m^{-1}, and that of PU from gray-black smoke was 0.139 m^{-1}. As these values represent the OD at the moment the detector was activated in repeated experiments, the results confirm that OD is closely related to the smoke particle color and the SSA. In other words, the white smoke generated from filter paper activates the detector at a relatively low OD value compared with those for kerosene and PU. Thus, the detector activation OD values, according to combustible, as presented in the figure, were applied directly to the calculation of the analysis criteria. Specifically, these dimensionless values were used for the OD of each, and generated and measured according to the combustible.

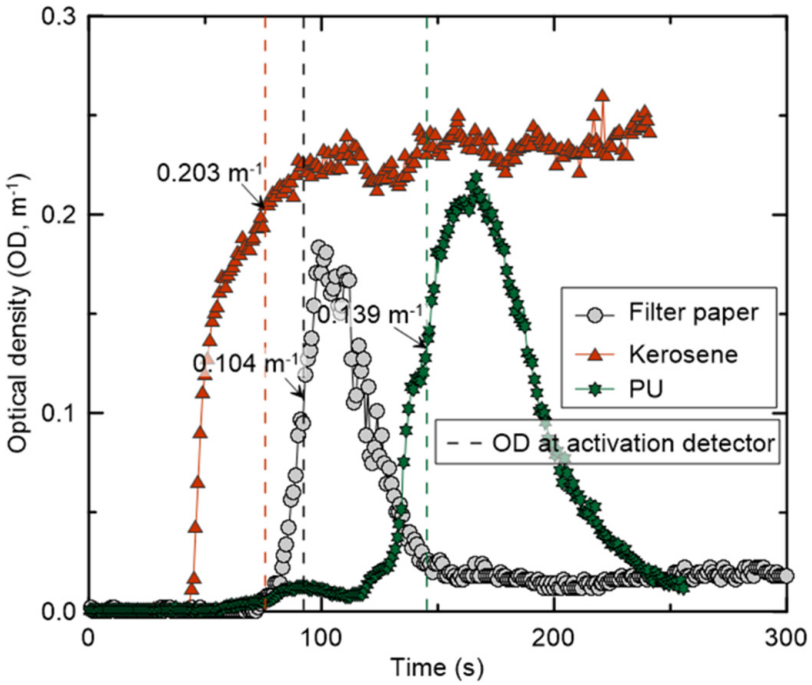


Figure 6. Detection of optical density through a smoke detector for each combustible.

Figure 7 shows the rate of change of the measured values from the initial values for the optical properties of each combustible by applying the analysis criteria presented in Table 1. Here, the x-axis ($OD/OD_{detector\ activation}$) is dimensionless, representing the moment activated OD was applied to all ODs measured in real time through repeated

experiments. Therefore, $x = 1$ represents the activation moment of the photoelectric smoke detector, $x < 1$ is the time before, and $x > 1$ is the time after. Figure 7a (criterion I) shows the ratio of the forward and backward scattering ratios to the 0° light extinction signal. For all the data plotted, the slope of the linear fit for filter paper is 0.2095, that for kerosene is 0.1261, and that for PU is 0.3091. Figure 7b shows the ratio of forward scattering to backward scattering by applying criterion II. The results confirm that filter paper has a value of 0.1755, kerosene a value of 0.0707, and PU a value of 0.2172. Finally, Figure 7c shows the ratio of light scattered to light extinction, to which criterion III is applied; the value for filter paper is 0.2109, that for kerosene is 0.1730, and that for PU is 0.2775. As described above, the slope for each type of combustible can be derived for the sections where data are plotted, and it can be confirmed that it is difficult to see a clear trend between combustibles. Therefore, as the plotted data are the result of minute voltages measured inside the LSC, it is necessary to clearly distinguish the relationship between the optical properties of the smoke particles generated from each combustible. Thus, it is reasonable to apply the data re-established through the zero resets of the initial value of the rate of change.

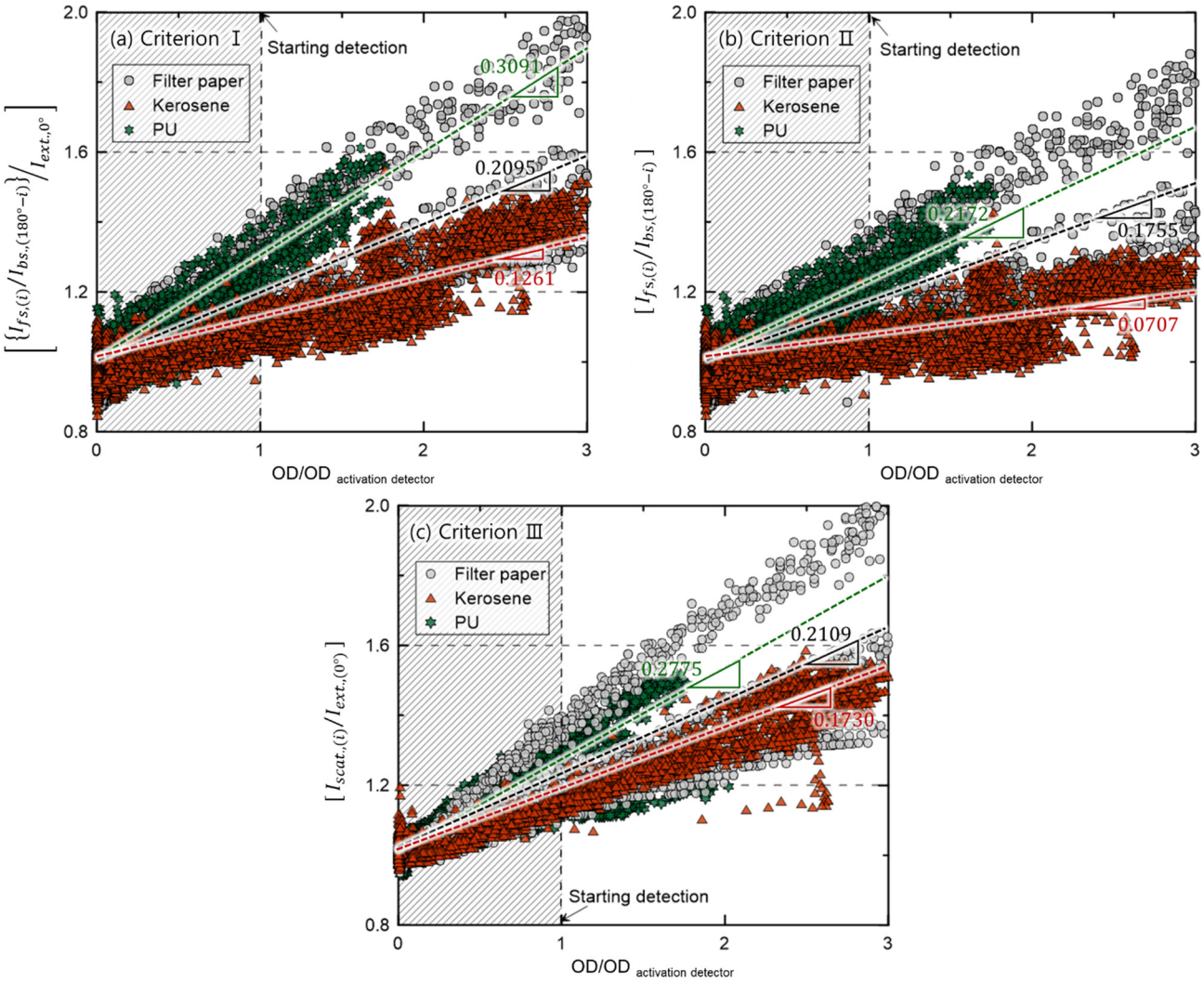


Figure 7. Comparison of results for the distribution of optical analysis criteria for the primary ratio according to the scattering angles ($I = 150°$).

Figure 8 shows the light scattering characteristics according to smoke particle color. The x-axis is dimensionless, representing the moment activation OD was applied to all OD values, measured in real time through repeated experiments. Therefore, $x = 1$ represents the moment of detector activation. The y-axis shows the ratio of the light-scattering signal, measured at all 11 detection angles installed inside the LSC, to the light extinction signal, measured at 0° (The detection angles of 15° to 165° for the scattering angle are represented via the values of index *j*, from 1 to 11). The results confirm that there is a distribution range for each combustible, excluding the initial smoke concentration when the combustible begins to burn. Specifically, filter paper exhibits a very wide distribution, with values ranging from 10 to 40, because light scattering is dominant for its smoke particles relative to those of the other combustibles. As a result, for kerosene and PU, corresponding to black and gray-black smoke, respectively, the ratio of the light scattering for all angles to the light extinction is relatively small.

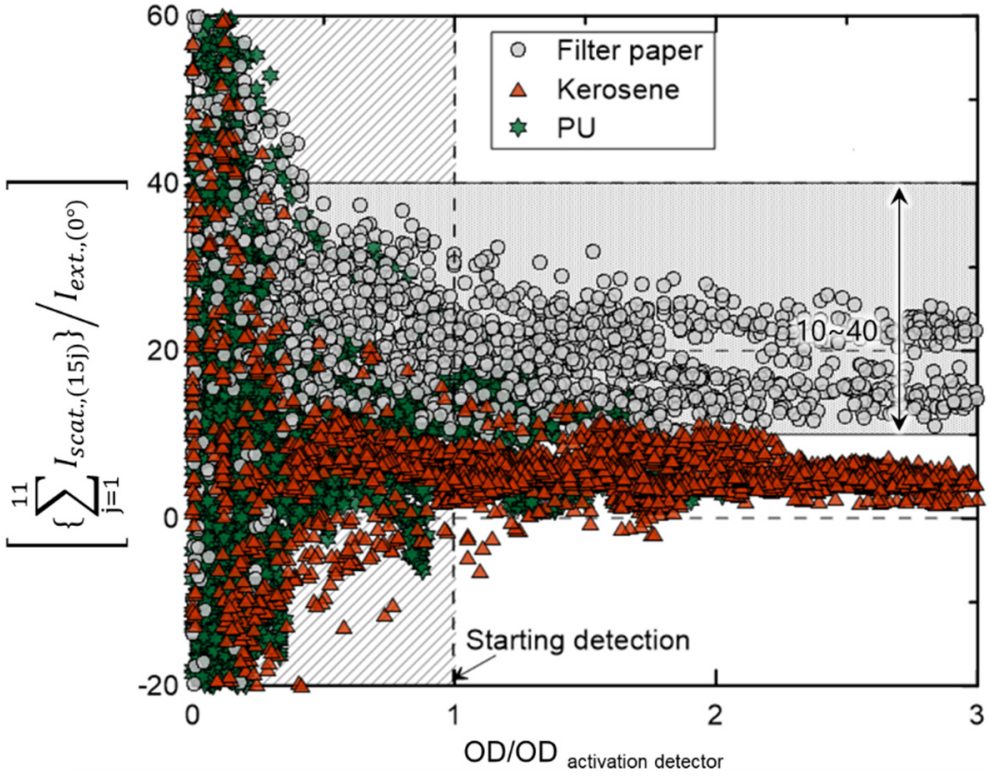


Figure 8. Distribution of ratios of light extinction and total light scattering according to combustibles.

Figure 9 shows the results obtained by applying criterion I (shown in Table 1). In Figure 9a, the y-axis represents the ratio of the forward and backward scattering ratio for 15°/165° to the 0° light extinction signal. The results confirm that for filter paper, as the OD increases, the value is included within the range of ±10. However, as this convergence occurs only after the detector is activated ($x > 1$), it cannot be considered differentiating data. In addition, as there is no such regularity in the results for the other combustibles, it is difficult to find meaning in the results or the method of analysis. Figure 9b shows the ratio of the forward and backward scattering ratios for 30°/150° to the 0° light extinction signal. Although this plot does not show a definite trend, the results obtained by analyzing each experiment confirm that the white smoke from filter paper has a positive value with a probability of 80%, as a negative signal was found in only 3 of 15 experiment repetitions. In the end, criterion I was deemed to have limited usefulness in distinguishing smoke colors through the distribution of light scattering and absorption signal measured inside the LSC.

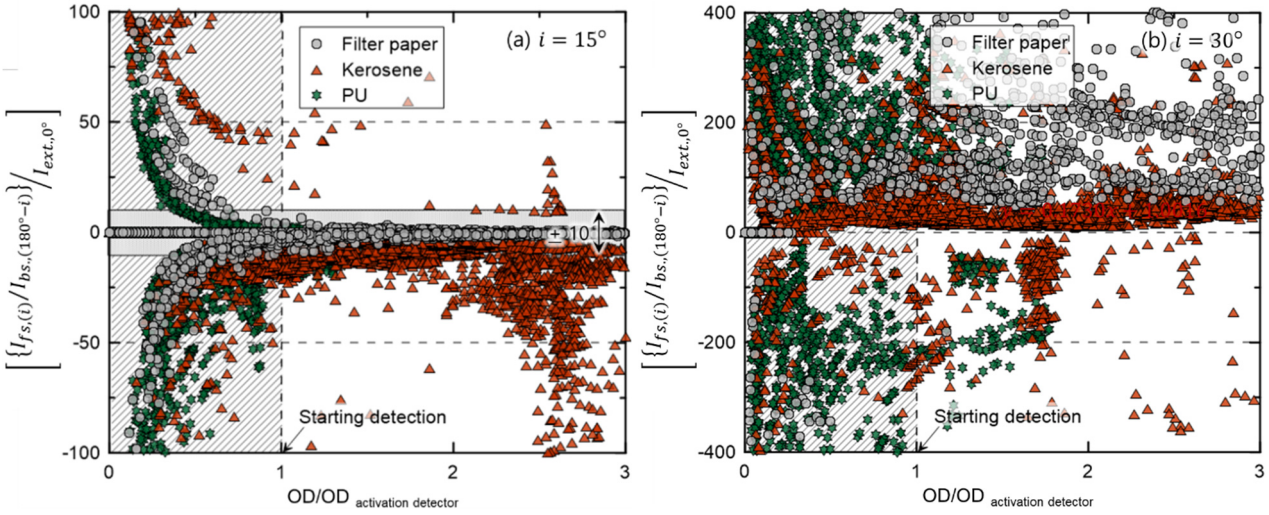


Figure 9. Example of insufficient results according to criterion I for the combustibles inside the chamber.

Figure 10 shows the asymmetry ratio results obtained by calculating the ratio of forward over backward scattering (criterion II). In Figure 10a, the y-axis represents the results, using 15° as the forward scattering angle and 165° as the backward scattering angle. The filter paper results are widely distributed in the shape of a sector symmetrical to $y = 0$. For kerosene, the values range from -5 to 0 from the initial point of smoke generation until after the activation of the photoelectric smoke detector. The signal for PU tends to appear at the same tendency as that for filter paper and kerosene. Therefore, if a signal falls outside the range from -5 to 0, it can be determined that it is not due to a smoke particle generated from kerosene. Figure 10b shows the ratio using 30° as the forward scattering angle and 150° as the backward scattering angle. The results confirm that the values for filter paper range from -0.5 to +0.5 as the OD increases; however, it is difficult to classify the data in the section before the moment of activation photoelectric smoke detector ($x < 1$), because they range relatively widely. Thus, criterion II is determined to be capable only of distinguishing kerosene, and only with signals measured at i = 15°.

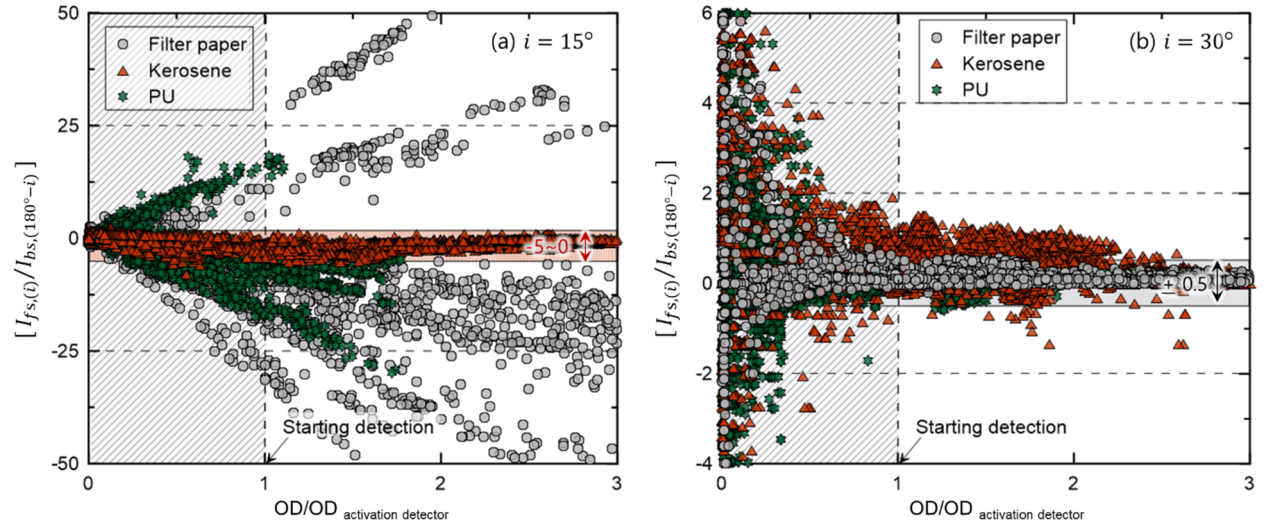


Figure 10. Comparison of results according to criterion II for the combustibles inside the chamber.

As criterion 3 is applied, Figure 11 shows the ratio through the measured signal of light extinction (0°) and light scattering (15°~165°) inside the LSC. The evaluation is based on the concept of SSA. Figure 11a shows the relationship between the signals for light

extinction (0°) and light scattered at 15°. The values for filter paper range from 2 to 7, and those for kerosene range from −2 to +2. As PU shares properties with both filter paper and kerosene, it exhibits no clear trend. As a result, ranges according to smoke color can be specified through post-processed data, except for cases in which there is almost no smoke. If the result is less than +2, smoke generated from filter paper (white smoke) is excluded, and if it exceeds +2, kerosene (black smoke) is excluded. Figure 11b shows the relationship between light extinguished (0°) and light scattered at 150°. The values for smoke generated from filter paper range from 5 to 20, and those for the smoke particles of kerosene range from 0 to 5. As before, a range for PU is difficult to distinguish clearly due to the characteristics of its gray-black smoke particles. It can be stated, however, that if a signal of less than five is derived through these results, it has a higher probability of corresponding to kerosene or PU than to filter paper. In this way, combustibles can be classified if the ranges in the figure are applied in combination according to the angle. That is, if the data measured in real-time are not included in the range, it can be an indicator for determining what color the smoke particles are in combustible material. These results are statistical and probabilistic, and it has been deemed to be feasible to classify the color of smoke generated from combustibles using a specific criterion and angle.

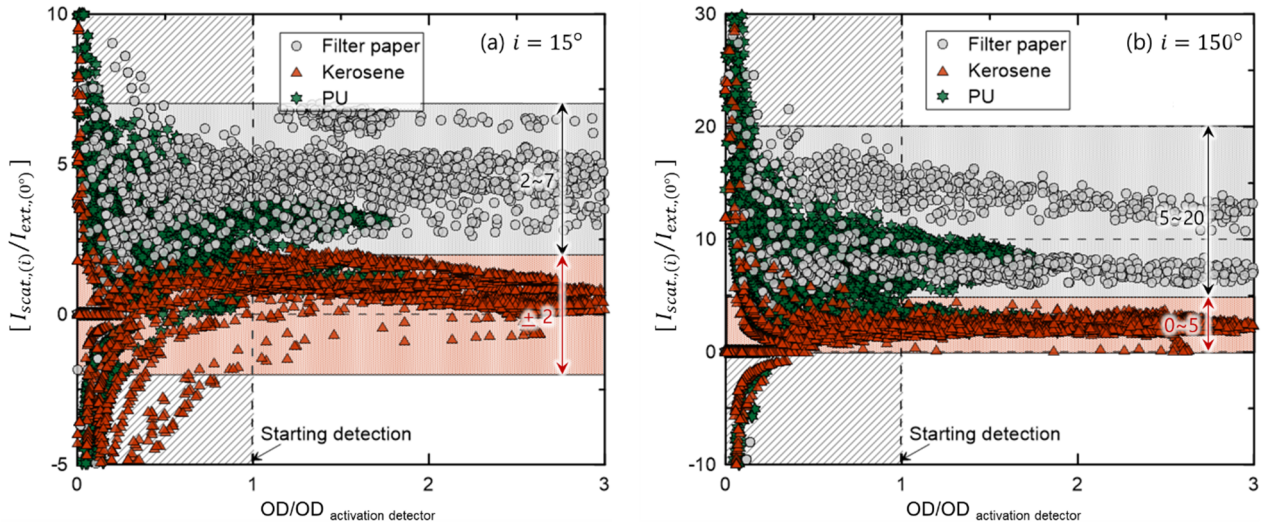


Figure 11. Comparison of results according to criterion III for the combustibles inside the chamber.

4. Conclusions

To address the inability of photoelectric smoke detectors to detect black smoke introduced in the same concentration as the white smoke used to control the detector's sensitivity, the optical characteristics of the smoke of various colors generated inside the detector chamber were analyzed. For this purpose, a light-scattering chamber (LSC) was constructed to have the simplified shape of the chamber of a photoelectric smoke detector. It contained one light-emitting unit, a light-extinction measuring unit (0°), and a scattered-light-receiving unit (11 angles, from 15° to 165° at 15° intervals). Filter paper, kerosene, and polyurethane (PU) were used as combustibles for smoke generation. The methods of analysis and the main results were as follows.

To investigate the distribution of the optical properties of smoke particles flowing into the LSC according to their color, three post-processing analysis criteria were applied to the measured light extinction and light scattering signals. Specifically, the asymmetry ratio—representing the ratio of forward scattering to backward scattering angles—was applied. In addition, in order to consider the single scattering albedo (SSA), which is affected by smoke color, the light extinction signal caused by the complex action of the light source and smoke particles was also considered.

The smoke particle size was roughly evaluated by examining the distribution of the scattering ratio, which was generated from each combustible material through a graph of the same scale as the cross-section inside the LSC. The relationship between the scattering angles and their initial values was examined first, because not all initial values measured by the light sensors were set identically. In addition, the slope was derived by applying a criterion according to the type of combustible used, and to confirm the relationship between the optical properties of the smoke particles, the data were re-established by applying a zero reset to ensure data validity.

The scattering signals were measured at all scattering angles for combustibles producing representative smoke colors, and were then analyzed using the analysis criteria. We found that it was possible to distinguish kerosene by using the asymmetry ratio at 15°/165°, and the results also suggest a way to distinguish between filter paper and kerosene by using a specific section of the values for 15°/0° and 150°/0°. When the specifically presented sections were applied in combination, a probabilistic indicator was presented to determine what color the smoke particles were in combustibles if the processed data were not included in the section.

In summary, light scattering distribution data were processed for reliability through repeated experiments for specific criteria and angles, and indicators (the ranges) were presented by which smoke colors could be distinguished probabilistically. This preliminary study has confirmed the interaction between smoke and a variety of variables. For the first step, the correlation between light and smoke particles was analyzed. As a follow-up study, it is expected that the operating characteristics of smoke detectors will be developed if an algorithm for distinguishing the light-scattering characteristics of various combustibles is prepared.

Author Contributions: Conceptualization, C.-H.H.; methodology, H.-Y.J. and C.-H.H.; validation, H.-Y.J. and C.-H.H.; formal analysis, C.-H.H.; investigation, H.-Y.J. and C.-H.H.; resources, C.-H.H.; data curation, H.-Y.J.; writing—original draft preparation, H.-Y.J.; writing—review and editing, C.-H.H.; visualization, H.-Y.J.; supervision, C.-H.H.; project administration, C.-H.H.; funding acquisition, C.-H.H. All authors have read and agreed to the published version of the manuscript.

Funding: This research was funded by the Institute of Information & Communications Technology Promotion (IITP) grant funded by the Korean government (MIST) (no. 2022-0-00012, Development of Intelligent Fire Detection Equipment Based on Smoke Particle Spectrum Analysis).

Institutional Review Board Statement: Not applicable.

Informed Consent Statement: Not applicable.

Data Availability Statement: Not applicable.

Conflicts of Interest: The authors declare no conflict of interest.

References

1. Lee, J.H.; Lee, C.H.; Kim, S.K.; Kong, H.S. A Study about False Alarm of Automatic Fire Detection System. *J. Korea Saf. Manag. Sci.* **2011**, *13*, 41–49. [CrossRef]
2. Cleary, T. Residential Nuisance Source Characteristics for Smoke Alarm Testing. To Be Determined. Available online: https://tsapps.nist.gov/publication/get_pdf.cfm?pub_id=861318 (accessed on 30 November 2022).
3. Liu, Z.; Kim, A.K. Review of Recent Developments in Fire Detection Technologies. *J. Fire Prot. Eng.* **2003**, *13*, 129–151. [CrossRef]
4. Reimann, P.; Schütze, A. Sensor arrays, virtual multisensors, data fusion, and gas sensor data evaluation. In *Gas Sensing Fundamentals*; Springer Series on Chemical Sensors and Biosensors; Kohl, C.D., Wagner, T., Eds.; Springer: Berlin/Heidelberg, Germany, 2013; Volume 15, pp. 67–107. [CrossRef]
5. Siebel, R. Test of Fire Detection Algorithms Using Artificially Generated Events. *Fire Saf. J.* **2006**, *41*, 258–265. [CrossRef]
6. Saeed, F.; Paul, A.; Hong, W.H.; Seo, H.C. Machine learning based approach for multimedia surveillance during fire emergencies. *Multimed. Tools Appl.* **2020**, *79*, 16201–16217. [CrossRef]
7. Panpaeng, S.; Phanpeang, P.; Metharak, E. Cigarette smoke detectors for non-smoking areas in the building. In Proceedings of the 2018 22nd International Computer Science and Engineering Conference (ICSEC), Chiang Mai, Thailand, 21–24 November 2018. [CrossRef]

8. National Standards of the Republic of Korea. *Detailed Inspection Regulations for Model Approval & Inspection Technical Standards for Fire Detectors*; Korea Fire Institute (KFI), National Fire Agency: Sejong-si, Republic of Korea, 2019; pp. 31–34.
9. Jang, H.Y.; Hwang, C.H. Obscuration Threshold Database Construction of Smoke Detectors for Various Combustibles. *Sensors* **2020**, *20*, 6272. [CrossRef]
10. Krishnan, S.S.; Lin, K.C.; Faeth, G.M. Extinction and Scattering Properties of Soot Emitted from Buoyant Turbulent Diffusion Flames. *J. Heat Transf.* **2001**, *123*, 331–339. [CrossRef]
11. Singh, S.; Fiddler, M.N.; Bililign, S. Measurement of Side-dependent Single Scattering Albedo of Fresh Biomass Burning Aerosols using the Extinction-Minus-scattering Technique with a Combination of Cavity Ring-down Spectroscopy and Nephelometry. *Atmos. Chem. Phys.* **2016**, *16*, 13491–13507. [CrossRef]
12. Jee, S.W. Analysis of the Response Time of a Photoelectric Spot-Type Smoke Detector Depending. *J. Korean Inst. Illum. Electr. Install. Eng.* **2013**, *27*, 89–94. [CrossRef]
13. Jee, S.W. A Study on the Fire Sources Analysis Using the Optical Characteristics of Smoke Particles and Neural Networks. *Korean Inst. Fire Sci. Eng.* **2014**, *28*, 64–70. [CrossRef]
14. Park, J.S.; Kim, D.K.; Choi, S.Y.; Lee, Y.S. Development of Flame and Smoke Detection for Early Fire Recognition. *J. Korean Inst. Fire Sci. Eng.* **2008**, *22*, 27–32.
15. Lee, H.S.; Kim, S.K. A Study on Response Characteristics of Photoelectric Type Smoke Detector Chamber Due to Dust Color. *Korean Inst. Fire Sci. Eng.* **2017**, *31*, 44–52. [CrossRef]
16. Miller, J.-T. Analyzing Photo-Electric Smoke Detector Response Based on Aspirated Smoke Detector Obscuration. Master's Thesis, University of Maryland, College Park, MD, USA, 2010. Available online: http://hdl.handle.net/1903/10455 (accessed on 22 March 2018).
17. Deng, T.; Wang, S.; Xiao, X.; Zhu, M. Eliminating the effects of refractive indices for both white smokes and black smokes in optical fire detector. *Sens. Actuators B Chem.* **2017**, *253*, 187–195. [CrossRef]
18. Wang, W.Q.; Pan, G.; Liu, X.L.; Wang, Y.Y.; Liu, Y.B.; Liu, B.; Jiang, L. Multi-angle Scattering Characteristic of test Fire Smoke and Typical Interference Aerosol. *Procedia Eng.* **2011**, *11*, 466–472. [CrossRef]
19. Xie, Q.; Zhang, H.; Wan, Y.; Zhang, Y.M.; Qiao, L.F. Characteristics of light scattering by smoke particles based on spheroid models. *J. Quant. Spectrosc. Radiat. Transf.* **2007**, *107*, 72–82. [CrossRef]
20. Keller, A.; Loepfe, M.; Nebiker, P.; Pleisch, R.; Burtscher, H. On-line determination of the optical properties of particles pro-duced by test fires. *Fire Saf. J.* **2006**, *41*, 266–273. [CrossRef]
21. Wang, S.; Xiao, X.; Deng, T.; Chen, A.; Zhu, M. A Sauter mean diameter sensor for fire smoke detection. *Sens. Actuators B Chem.* **2019**, *281*, 920–932. [CrossRef]
22. Weinert, D.W.; Cleary, T.; Mulholland, G.W.; Beever, P.F. Light Scattering Characteristics and Size Distribution of Smoke and Nuisance Aerosols. In Proceedings of the 7th International Symposium on Fire Safety Science, Gaithersburg, MD, USA, 16–21 June 2003; pp. 209–220. Available online: https://tsapps.nist.gov/publication/get_pdf.cfm?pub_id=861092 (accessed on 10 August 2022). [CrossRef]
23. Weinert, D.; Cleary, T.; Mulholland, G. *Size Distribution and Light Scattering Properties of Test Smokes (NIST SP 965)*; Special Publication (NIST SP); National Institute of Standards and Technology: Gaithersburg, MD, USA, 2001. Available online: https://tsapps.nist.gov/publication/get_pdf.cfm?pub_id=912274 (accessed on 20 September 2022). [CrossRef]
24. Deng, T.; Zeng, J.; Wang, S.; Uan, S.; Chen, A. An optical fire detector with enhanced response sensitivities for black smokes based on the polarized light scattering. *Meas. Sci. Technol.* **2019**, *30*, 115203. [CrossRef]
25. Jun, L.S.; Peng, L. Vertical Two-Way Dispersion Smoke Sensing Detector Labyrinth. CN Patent 1987426A, 23 December 2005.
26. James, R.; Louis, D.; Jayanthi, P. Smoke Chamber. U.S. Patent 6778091, 17 August 2004.
27. Butler, K.M.; Mulholland, G.W. Generation and Transport of Smoke Components. *Fire Technol.* **2004**, *40*, 149–176. [CrossRef]
28. Léonard, S.; Mulholland, G.W.; Puri, R.; Santoro, R.J. Generation of CO and Smoke During Underventilated Combustion. *Combust. Flame* **1994**, *98*, 20–34. [CrossRef]
29. Mulholland, G.W.; Johnsson, E.L.; Fernandez, M.G.; Shear, D.A. Design and testing of new smoke concentration meter. *Repr. Fire Mater.* **2000**, *24*, 231–243. [CrossRef]
30. Kim, B.J.; Cho, J.H.; Hwang, C.H.; Park, S.H. A study on the development of a low-cost device for measuring the optical smoke density. *Korean Inst. Fire Sci. Eng.* **2015**, *29*, 81–88. [CrossRef]
31. Hulst, H.C. *Light Scattering by Small Particles*; John Wiley and Sons: New York, NY, USA; Chapman and Hall: London, UK, 1981; p. 470. [CrossRef]
32. Holland, A.C.; Alfred, C.; Gagne, G. The Scattering of Polarized Light by Polydisperse Systems of Irregular Particles. *Appl. Opt.* **1970**, *9*, 1113–1121. [CrossRef] [PubMed]
33. Costea, A.; Schiopu, P. New design and improved performance for smoke detector. In Proceedings of the 2018 10th International Conference on Electronics, Computers and Artificial Intelligence (ECAI), Lasi, Romania, 28–30 June 2018; pp. 1–7. [CrossRef]
34. Zheng, R.; Cheng, Y.; Zhang, H. A Study on Scattering Characterization of Water Steam Aerosols for Smoke Detector. In Proceedings of the 2017 Suppression, Detection, and Signaling Research and Applications Conference (SUPDET 2017) Was Jointly Organized with the 16th International Conference on Fire Detection (AUBE '17), College Park, MD, USA, 12–14 September 2017.

35. Howell, J.R.; Mengüç, M.P.; Daun, K.; Siegel, R. *Thermal Radiation Heat Transfer*, 7th ed.; CRC Press: Boca Raton, FL, USA, 2020; Chapter 15; pp. 682–740. [CrossRef]
36. Jobert, G.; Barritault, P.; Fournier, M.; Boutami, S.; Jobert, D.; Marchant, A.; Michelot, J.; Monsinjon, P.; Lienhard, P.; Nicoletti, S. Miniature particulate matter counter and analyzer based on lens-free imaging of light scattering signatures with a holed image sensor. *Sens. Actuators Rep.* **2020**, *2*, 100010. [CrossRef]

Disclaimer/Publisher's Note: The statements, opinions and data contained in all publications are solely those of the individual author(s) and contributor(s) and not of MDPI and/or the editor(s). MDPI and/or the editor(s) disclaim responsibility for any injury to people or property resulting from any ideas, methods, instructions or products referred to in the content.